

## Rapidly variable Fe $K\alpha$ line in NGC 4051

J.X. Wang<sup>1</sup>, Y.Y. Zhou<sup>1,3,4</sup>, H.G. Xu<sup>2</sup>, T.G. Wang<sup>1,5</sup>

Received \_\_\_\_\_; accepted \_\_\_\_\_

---

<sup>1</sup>Center for Astrophysics, University of Science and Technology of China, Hefei, Anhui, 230026, P. R. China; jxw@mail.ustc.edu.cn

<sup>2</sup>Institute for Space Astrophysics, Department of Physics, Shanghai Jiao Tong University, Shanghai, 200030, P. R. China

<sup>3</sup>Beijing Astrophysics Center, Beijing, 100080, P. R. China

<sup>4</sup>Laboratory of Cosmic Ray and High Energy Astrophysics, Chinese Academy of Sciences, Beijing, 100039, P. R. China

<sup>5</sup>The Institute of Physical and Chemical Research (RIKEN), 2-1, Horosawa, Wako, Saitama, 351-0198, Japan

## ABSTRACT

We present a detailed analysis on the variability of the Fe K emission line in NGC 4051 using ASCA data. Through simple Gaussian line fits, we find not only obvious Fe K line variability with no significant difference in the X-ray continuum flux between two ASCA observations which were separated by  $\sim 440$  days, but also rapid variability of Fe K line on time scales  $\sim 10^4$  s within the second observation. During the second observation, the line is strong (EW =  $733_{-219}^{+206}$  eV) and broad ( $\sigma = 0.96_{-0.35}^{+0.49}$  keV) when the source is brightest, and become weaker (EW =  $165_{-86}^{+87}$  eV) and narrower ( $\sigma < 0.09$  keV) whilst the source is weakest. The equivalent width of Fe K line correlates positively with the continuum flux, which shows an opposite trend with another Seyfert 1 galaxy MCG -6-30-15.

*Subject headings:* galaxies: individual (NGC 4051) — galaxies: Seyfert — X-rays: galaxies

## 1. Introduction

It has long been recognized that measurement of the profile of the Fe K $\alpha$  fluorescence line found in many AGNs at  $\sim 6.4$  keV (Mushotzky 1995, Tanaka et al. 1995, Yaqoob et al. 1995, Fabian et al. 1995, Nandra et al. 1997a and references therein) can provide an important tracer of matter in the vicinity of the postulated supermassive black hole. Doppler and gravitational shifts would imprint characteristic signatures on the line profile which map the geometric and dynamical distributions of matter surround the black hole. Additional information concerning the geometry of matter in the active nucleus could in principle be derived by studying the rapid variability of the line profile, intensity and their relationship with the continuum variations. So far, rapid variability in Fe K line has been detected only in two Seyfert galaxies.

Yaqoob et al. (1996) presented the evidence for rapid variability of the Fe K line profile in the narrow-line Seyfert galaxy NGC 7314, which is consistent with a diskline of constant equivalent width superposed on a constant flux narrow line (presumably from the torus). They found while the X-ray continuum flux varied by a factor of 2 on a time scale of hundreds of seconds, the emission in the red wing of the Fe K line below  $\sim 6$  keV responded to those variations on the time scales of less than  $\sim 3 \times 10^4$  s, and the response becomes slower and slower towards the line peak near 6.4 keV. Rapid variability of the Fe K line profile was also found in the bright Seyfert 1 galaxy MCG -6-30-15 (Iwasawa et al. 1996). On time scales of less than  $\sim 10^4$  s, the variability pattern is the same as seen in NGC 7314. But on long time scales of about several  $10^4$  s, it shows a different behavior. When the source is bright, the Fe K line is weak and dominated by the narrow core, whilst during a deep minimum, a huge red tail appears. The intensity of broad Fe K line correlates inversely with the continuum flux, so does the equivalent width.

In this Letter we present an evidence of rapid variability of Fe K line in another nearby

( $Z = 0.0023$ ) low luminosity narrow-line Seyfert 1 galaxy NGC 4051, which is well known for its rapid variability in the X-ray band. Nandra & Pounds (1994) found an equivalent width of Fe K line  $140 \pm 70$  eV from the Ginga data by assuming a single narrow line. A narrow Fe K emission line was also detected with an upper limit on the FWHM of  $\sim 460$  eV and equivalent width  $EW \sim 170$  eV during the first ASCA observation in 1993 (Mihara et al. 1994, hereafter M94) for this object. When the target was re-observed by ASCA in 1994 (Guainazzi et al. 1996, hereafter G96), the Fe K line was found to be stronger ( $EW = 350_{-150}^{+170}$  eV) and broad ( $\sigma > 0.2 keV$ ).

## 2. The ASCA data

NGC 4051 was observed twice by ASCA from 1993 April 25 22:30 to April 26 21:30 and from 1994 July 6 15:28 to July 9 10:40. In this Letter, we concentrated on the Solid-state Imaging Spectrometer (SIS) data because of the better energy resolution it provides (Inoue 1993). The data reductions were performed with the ASCA standard software XSELECT according to the following criteria: satellite not passing through the South Atlantic Anomaly, geomagnetic cutoff rigidity greater than  $6 \text{ GeVc}^{-1}$ , and minimum elevation angle above Earth's limb of  $10^\circ$  and  $20^\circ$  for nighttime and daytime observations, respectively. Source counts were extracted from a circular area of radius  $4'$  for the SIS0 and SIS1. Because of an error in satellite pointing during the first observation, the image fell into the dead region between two chips in SIS1 (M94). Therefore we only used SIS0 data from this observation for spectral analysis. To avoid the complexity caused by the "warm absorber" and "soft excess" (M94, G96), we use the 2.5–10.0 keV data for spectral analysis. Spectral fits were carried out using the XSPEC, and the background was taken from the blank sky data.

### 3. Variability of Iron K Line

#### 3.1. Comparisons between two observations

Time average spectra of Fe K $\alpha$  line profiles for the two observations were given by Nandra et al. (1997a) & G96. Due to the poor statistics, the line profile cannot be measured exactly, therefore we model the line with a single Gaussian function. The underlying continuum is fitted with a single power-law absorbed by the Galactic column density ( $N_H \approx 1.3 \times 10^{20} \text{ cm}^{-2}$ ). We did not take into account of the possible Compton reflection component here because of its small impact on the ASCA spectra.

Results of the single Gaussian fits are given in Table 1. For comparison, the results of diskline (Fabian et al. 1989, George & Fabian 1991) fits can be found in Nandra et al. (1997a) & G96. The variability of Fe K line is evident (EW changes from 166 eV to 330 eV and FWHM from 4500 km/s to 50000 km/s), however, there is no obvious variability in the photon index of X-ray continuum. Because of the pointing error of the satellite during the first observation, part of the photons fell into the gaps between the CCD chips. The continuum flux of Obs1 in Table 1 is only a lower limit. However, since the gaps occupy a fairly small fraction of the selected area that includes our target ( $\sim 18\%$ ), the continuum flux obtained cannot be biased too much. Thus we conclude that there is no significant difference in the continuum flux between two observations.

#### 3.2. Rapid FeK Line variability in the second observation

During the two ASCA observations, NGC 4051 shows large amplitude X-ray continuum flux changes on time scales of  $\sim 100$  s. In order to see if there are short time scale variations of Fe K line within a single observation, we choose Obs2 which last longer time ( $\sim 3$  days) for analysis in detail. Including a large flare in the beginning and a deep minimum near the

end, the whole observation has been divided into five time intervals (from i1 to i5) with a similar exposure time ( $\sim 10$  ks) as shown in Fig. 1 (different from G96). Among the five intervals, i-2, i-3, i-4 have similar continuum fluxes.

Results of single Gaussian fittings are shown in Table 1 (We also give the results of diskline fits to the five intervals, respectively). The photon index is quite similar between i2 to i4 at about  $\Gamma \sim 1.80$ . A steeper continuum is suggested for i-1 and a flatter one for i-5. The single Gaussian line dispersions and equivalent widths are also similar between i2 to i4. A stronger and broader line is detected in i-1, and a weaker narrower one in i-5 (Fig. 2). In order to show the variability of Fe K line more clearly, we present a contour plot of Gaussian line width versus the equivalent width for i-1, i-5 and i-2+3+4 (a summed dataset of i-2,i-3,i-4) obtained from the single Gaussian fits in Figure 3. For i-1, the equivalent width of Fe K line is 733 eV, much larger than that for the time average spectrum, and the Fe K line is much broader ( $\sigma = 0.96$  keV). While for i-5, the EW of Fe K line is only 165 eV, and much narrower (only a narrow line has been detected,  $\sigma < 0.09$  keV). Due to the poorer statistics in i-5, there is concerning that a weak broad Fe K component might be un-noticeable. To exclude this possibility, we add a broad Gaussian line ( $E_G = 6.4$  keV,  $\sigma = 0.46$  keV, the same with the time average spectrum) to the fit. The upper limit for the EW of this component is 80 eV, far smaller than those in i-1 to i-4. These results clearly demonstrate the large variability of Fe K line during the second ASCA observation. G96 also analyzed the Fe K line, but failed to detect the variability of Fe K line profiles and equivalent widths. We would like to point out here that the time sequence selection used in G96, different to what we did in this paper, tends to smear out the line variations.

#### 4. Discussions

#### 4.1. The X-ray continuum flux versus the equivalent width of Fe K line

We detect significant change not only in line equivalent width but also in line profile through single Gaussian fitting to the two observations. From 1993.4.25 to 1994.7.6, Fe K line in NGC 4051 became broader and stronger, in spite of the fact the continuum flux remains almost constantly. This shows that the long time scale variability of Fe K line can be independent of the continuum variation. Such kind of behavior can be induced by the change in structure of the line emission region or the geometry of the hard X-ray source in the context of disk line model. The broader and stronger line emission during the 1994 epoch indicates that the average line emission region is much closer to the putative accretion disk. We also detect rapid variability ( $\sim 10^4$ s) of Fe K line within the second observation. During the bright flare (i-1), the Fe K line is broad and strong, while during the deep minimum (i-5), Fe K line is narrower and weaker.

Using the ASCA data of 39 AGNs, Nandra et al. (1997b) found a clear decrease in the strength of the Fe K $\alpha$  line with the increase in the luminosity (X-ray Baldwin effect, Iwasawa & Taniguchi 1993), which was thought due to the fact that high-luminosity AGNs have high accretion rates, causing the accretion disk to become ionized (Matt et al. 1996). An inverse correlation between the Fe K line EW and the X-ray continuum flux was also found in MCG –6-30-15. The line EWs (sum of the broad and narrow component, calculated at the centroid energy 6.4 keV, see Table 2, Iwasawa et al. 1996) versus continuum flux is plotted here in Fig. 4b. The case for the NGC 4051 shows that the situation is more complicated than this. We find an increase in the equivalent width with no apparent change in the continuum flux when the two ASCA observations are considered. Moreover, an increase in the line EW with the increase X-ray continuum flux (Fig. 4a), completely opposite to the Baldwin effect and the variability in MCG –6-30-15, is found during the second ASCA observation. It indicates a complicate mechanism should be considered.

#### 4.2. rapid variability on time scale $\sim 10^4$ s

It is well known that the X-ray source in many AGNs is highly variable on short time scales  $\sim 100$  s. As Fe K line is produced via fluorescent process, its strength and profile should respond to the continuum variability. Obviously, the measurement of the temporal response is the best way to map the matter distribution in innermost regions around the black hole. In principle, the distance from the X-ray continuum source to the line emission region could be determined through observing reverberation effect (Reynolds et al. 1998). With the Fe K line profile, we could derive the mass of the black hole in the heart of nucleus. The characteristic time scales on which reverberation effects occur is the light crossing time of one gravitational radius, which is  $\sim 50$  s for a  $10^7 M_{\odot}$  black hole. But, all current available instruments are not able to measure such a fast time response. Even for a bright Seyfert galaxy, ASCA can only obtain 1~2 Fe K line photons in 100 s, too few to define the line flux and profile. However, the Fe K line variability of time scales  $\sim 10^4$  s can provide constraints on the long time scale ( $\sim 10^4$  s) variation of the X-ray source or the line emission region. So far, such variability has been detected in only three Seyfert galaxies, NGC 7314, MCG –6-30-15 and NGC 4051. For NGC 7314, a simple disk-plus-torus model could explain its rapid variability fairly well. But for MCG –6-30-15 and NGC 4051, the situation is more complicated.

According to the disk model, the fluorescent iron lines are produced from the hard X-ray irradiation of the disk composed of cold gas around a black hole. When the X-ray source is bright, iron will start to be ionized, and in the intermediate ionization states, the resonance scattering can cause a reduction in the line flux (Matt et al. 1996). It is a possible reason causing the anti-correlation of the EW of broad components to the X-ray continuum flux in MCG –6-30-15. We consider that the ionized disk is also a possible reason for the positive correlation in NGC 4051 because a factor  $\sim 2$  larger EW for FeXXV than cold iron could



occur (Matt et al. 1996). Though not well constrained, the diskline energies for i1 to i5 in Table 1. show an trend to correlate with the continuum flux, which gives some support to this opinion.

There is also another possible explanation to the the rapid variability of Fe K line. Fabian (1997) suggested that the X-ray continuum might be generated by magnetic flares above the accretion disk. At any given time there are only a few flares otherwise the rapid variability will be average out. When the dominated flares move around on the disk, changes in the Fe K line profile would be seen. Such model could explain the odd variability of Fe K line in MCG –6-30-15 well. We think it is also appropriate for the rapid variability in NGC 4051 discovered in this paper. For the sequence i-5, the Fe K line profile is similar to the bright flare in MCG –6-30-15. The small FWHM might due to a dominate flare located far away from the central black hole, or a succession of flares on the approaching side of the disk. The broad line during i-1 might due to a bright dominate flare very close ( $\sim 6R_g$ ) to the black hole, and the large EW might due to a overabundance of iron.

This work is supported by Chinese National Natural Science Foundation, PanDeng Project and Foundation of Ministry of Education. The authors would also like to thank S.A. Huang for great help with ASCA data reduction.

## REFERENCES

- Fabian A.C., Rees M.J., Stella L. & White N.E. 1989, MNRAS, 238, 729
- Fabian A.C., Nandra K., Reynolds C.S., Brandt W.N., Otani C., Tanaka Y., Inoue H., Iwasawa K. 1995, MNRAS, 277, L11
- Fabian A.C. 1997, X-ray Imaging and Spectroscopy of Cosmic Hot Plasmas, Univ. Acad. Press, 201
- George I.M. & Fabian A.C. 1991, MNRAS, 249, 352
- Guainazzi M., Mihara T., Otani C. & Matsuoka M., 1996, PASJ, 48, 781 (G96)
- Inoue H. 1993, Exp.Astro., 4, 1
- Iwasawa K. & Taniguchi Y. 1993, ApJ, 413, L15
- Iwasawa K., Fabian A.C., Reynolds C.S., Nandra K., Otani C., Inoue H., Hayashida K., Brandt W.N., Dotani T., Kunieda H., Matsuoka M. & Tanaka Y. 1996, MNRAS, 282, 1038
- Matt G., Fabian A. C. & Ross R. R. 1996, MNRAS, 278, 1111
- Mihara T., Matsuoka M., Mushotzky R.F., Kunieda H., Otani C., Mitamoto S. & Yamauchi M. 1994, PASJ, 46, L137 (M94)
- Mushotzky R.F., Fabian A.C., Iwasawa K., Kunieda H., Matsuoka M., Nandra K., Tanaka Y. 1995, MNRAS, 272, L9
- Nandra K. & Pounds K.A. 1994, MNRAS, 268, 405
- Nandra K., George I.M., Mushotzky R.F., Turner T.J. & Yaqoob T. 1997a, ApJ, 477, 602
- Nandra K., George I.M., Mushotzky R.F., Turner T.J. & Yaqoob T. 1997b, ApJ, 488, L91
- Reynolds C.S., Young A.J., Begelman M.C. & Fabian A.C. 1998, 0 to ApJ, ASTROPH-9806327

Tanaka Y., Nandra K. Fabian A.C., Inoue H., Otani C., Dotani T., Hayashida K., Iwasawa K., Kii T., Makino F., Matsuoka M. 1995, *Nature*, 375, 659

Yaqoob T., Edelson R., Weaver K.A., Warwick R.S., Mushotzky R.F., Serlemitsos P.J., Holt S.S. 1995, *ApJ*, 453, L81

Yaqoob T., Serlemitsos P.J., Turner T.J., George I.M. & Nandra K. 1996, *ApJ*, 470, L27

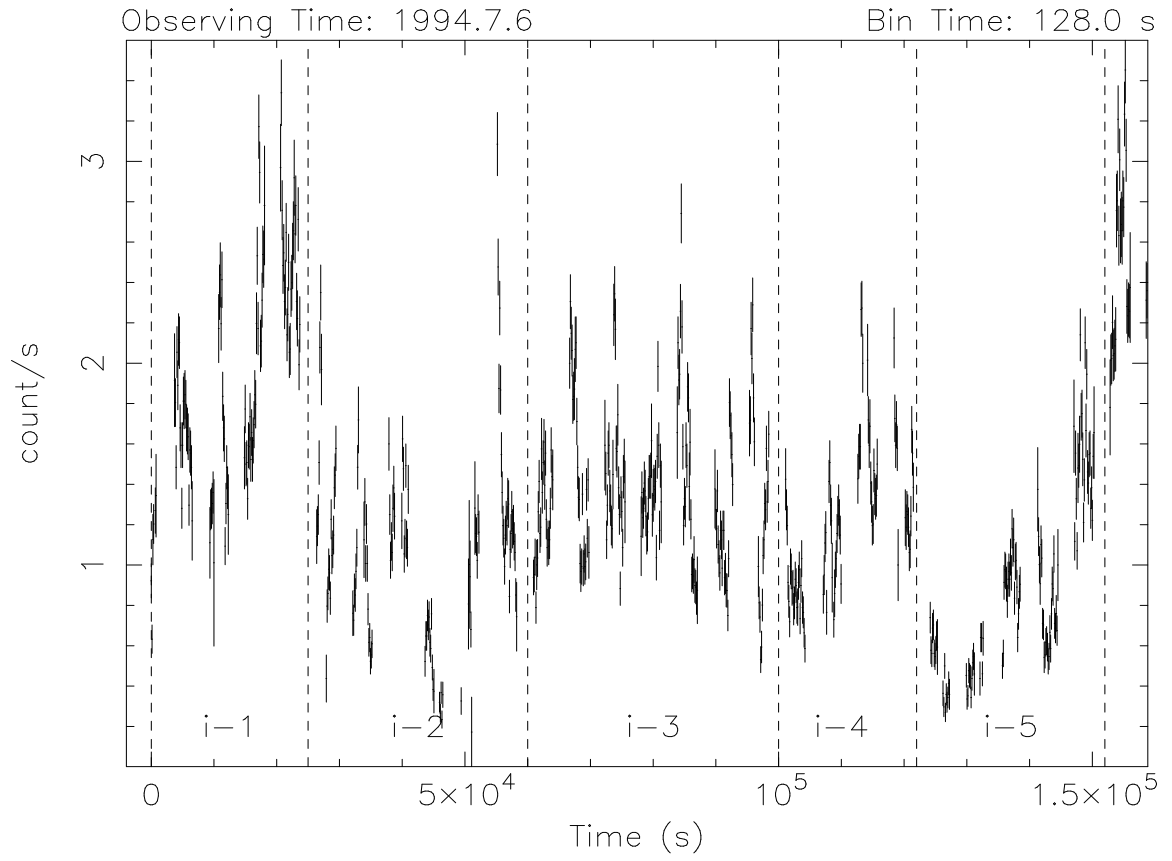


Fig. 1.— The 0.4–10.0 keV light curve from the SIS0 for the second ASCA observation, binned at 128 s. Time-intervals used in the section 3.2 are also indicated here.

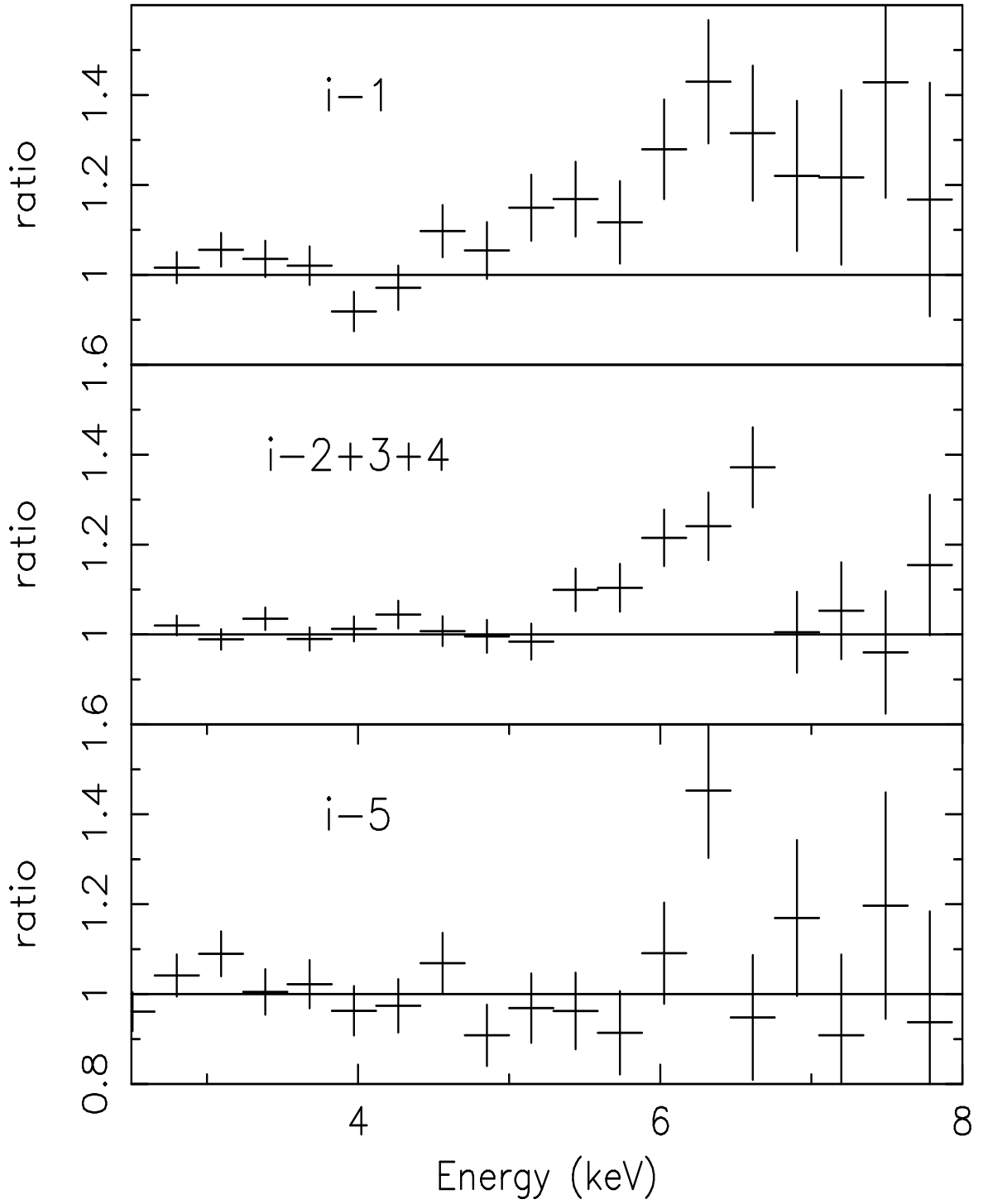


Fig. 2.— Ratios of the data to an absorbed power-law model fit to the data in the 2.5 to 4.5 keV and 7.0 to 10.0 keV bands to illustrate the Fe K line profile for the SIS in the time intervals  $i-1, i-2+3+4, i-5$ , which are indicated in Fig. 1.

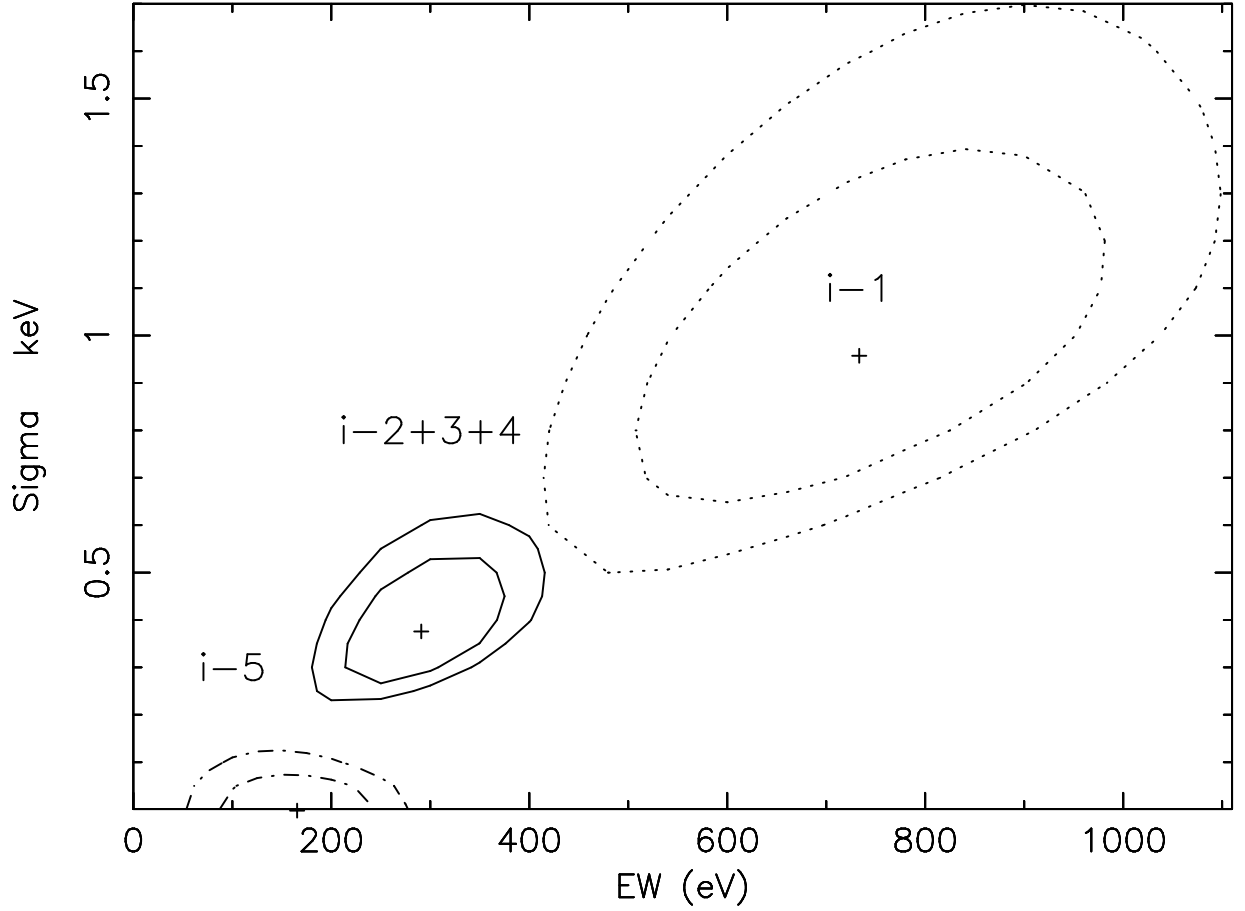


Fig. 3.— 68 and 90 per cent contours in the line width and the line EW for two degrees of freedom from the single Gaussian fit to the spectra in the time-intervals  $i-1, i-2+3+4, i-5$ .

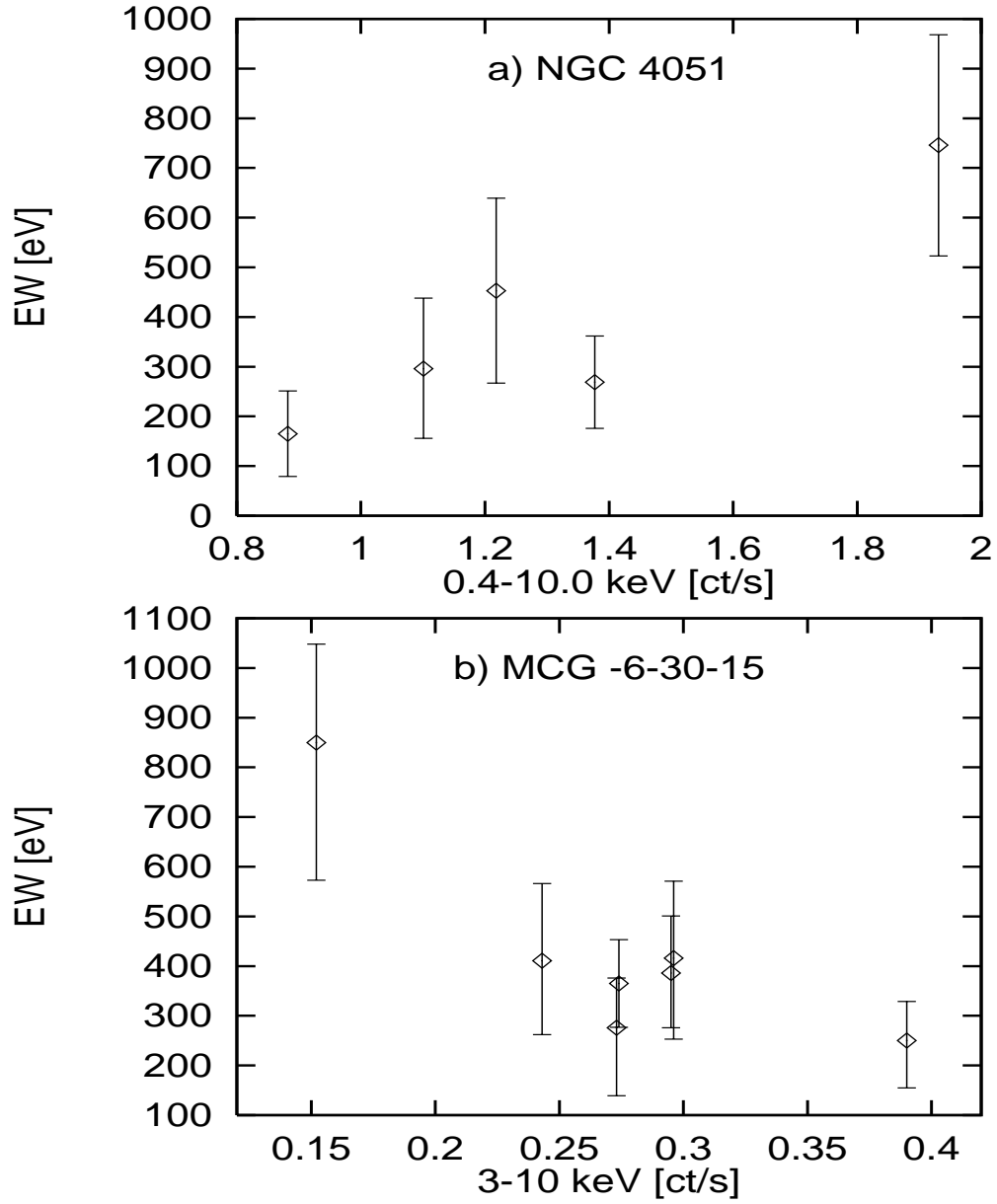


Fig. 4.— Plot of Fe K line EWs versus continuum flux for: a) NGC 4051 and b) MCG -6-30-15.

Table 1: Single Gaussian fits to the two ASCA observations and the five datasets of Obs2

...	$\Gamma^a$	$E_G$ (keV)	$\sigma$ (keV)	EW (eV) <sup>c</sup>	$\chi^2/dof$	flux <sup>b</sup>	$E_D^d$ (keV)	$R_i/R_g^d$
Obs1	$1.94^{+0.12}_{-0.11}$	$6.49^{+0.05}_{-0.16}$	$0.04^{+0.14}_{-0.04}$	$162^{+72}_{-72}$	148/127	> 2.15		
Obs2	$1.83^{+0.05}_{-0.06}$	$6.35^{+0.14}_{-0.14}$	$0.46^{+0.19}_{-0.14}$	$330^{+68}_{-68}$	308/335	2.42		
i-1	$2.04^{+0.13}_{-0.13}$	$6.45^{+0.44}_{-0.44}$	$0.96^{+0.49}_{-0.35}$	$733^{+206}_{-219}$	184/190	...	$6.74^{+0.30}_{-0.40}$	$6.3^{+2.4}_{-0.3}$
i-2	$1.71^{+0.14}_{-0.13}$	$6.02^{+0.28}_{-0.38}$	$0.44^{+0.21}_{-0.18}$	$296^{+142}_{-140}$	174/172	...	$6.49^{+0.11}_{-0.11}$	$13.^{+11.}_{-6.}$
i-3	$1.83^{+0.10}_{-0.10}$	$6.47^{+0.19}_{-0.13}$	$0.21^{+0.34}_{-0.13}$	$269^{+93}_{-93}$	228/227	...	$6.49^{+0.11}_{-0.11}$	$13.^{+11.}_{-6.}$
i-4	$1.87^{+0.16}_{-0.17}$	$6.18^{+0.31}_{-0.29}$	$0.46^{+0.94}_{-0.27}$	$453^{+186}_{-186}$	119/138	...	$6.61^{+0.16}_{-0.15}$	$7.0^{+4.1}_{-0.9}$
i-5	$1.51^{+0.15}_{-0.15}$	$6.39^{+0.05}_{-0.05}$	$0.00^{+0.09}_{-0.00}$	$165^{+87}_{-86}$	152/149	...	$6.40^{+0.07}_{-0.09}$	$999^{+1}_{-787}$

<sup>a</sup>Best fitting value when data in 4.5-7.0 keV region are excluded

<sup>b</sup>  $\times 10^{-11} \text{erg.cm}^{-2}.\text{s}^{-1}$  (2-10 keV)

<sup>c</sup>calculated at the centroid energy 6.4 keV

<sup>d</sup>Results of diskline models fits with disk emissivity index  $q$  fixed at -3.0, the outer disk radii  $R_o$  at  $1000R_g$  ( $R_g = GM/c^2$ ) and the inclination of the disk at  $25^\circ$  (G96)